Elastic anisotropy of FeSiO$_3$ end-members of the perovskite and post-perovskite phases

Stephen Stackhouse, John P. Brodholt, and G. David Price

Department of Earth Sciences, University College London, London, UK

[1] The athermal elastic constants of the perovskite and post-perovskite polymorphs of pure end-member FeSiO$_3$ were calculated from ab initio calculations. We predict that incorporating ten mole percent FeSiO$_3$ together with four mole percent Al$_2$O$_3$ into MgSiO$_3$ reduces the perovskite to post-perovskite phase transition pressure by 5 GPa. Small changes in the seismic properties of the post-perovskite phase due to the incorporation of iron and alumina are compatible with observations for the lower mantle. MgSiO$_3$ post-perovskite enriched in fifty percent or more iron may be responsible for ultra-low velocity zones at the base of the mantle. Citation: Stackhouse, S., J. P. Brodholt, and G. D. Price (2006), Elastic anisotropy of FeSiO$_3$ end-members of the perovskite and post-perovskite phases, Geophys. Res. Lett., 33, L01304, doi:10.1029/2005GL023887.

1. Introduction

[2] The core-mantle boundary is overlain by a distinct layer a few hundred kilometers thick that acts as a thermal and compositional boundary, separating the predominantly silicate solid lower mantle from the hotter molten iron outer core [Lay et al., 2004]. This layer, referred to as D$''$, exhibits unusual seismic features, such as a discontinuity at the top in some parts [Sidorin et al., 1999], shear-wave splitting [Panning and Romanowicz, 2004], anti-correlation of bulk and shear sound speeds [Su and Dziewonski, 1997] and ultra-low velocity zones [Garnero and Helmberger, 1995]. The recently reported post-perovskite phase transition in pure end-member MgSiO$_3$ [Murakami et al., 2004; Shim et al., 2004] offers a potential explanation for these, with theoretical studies showing that the stability field and elastic properties of the post-perovskite phase could produce seismic features compatible with observations [Iitaka et al., 2004; Oganov and Ono, 2004; Tsuchiya et al., 2004; Stackhouse et al., 2005a]. The lower mantle, however, does not consist of pure MgSiO$_3$, but is expected to incorporate about four mole percent Al$_2$O$_3$ [Anderson, 1989] and approximately ten mole percent FeSiO$_3$ [Wood and Rubie, 1996]. Theoretical studies [Caracas and Cohen, 2005; Stackhouse et al., 2005b] suggest that incorporation of a few mole percent aluminum into pure MgSiO$_3$ would increase the perovskite to post-perovskite phase transition pressure by less than 1 GPa and have little effect on the seismic properties of the post-perovskite phase. In contrast, experimental work [Mao et al., 2004] suggests that iron preferentially enters the post-perovskite phase of MgSiO$_3$ relative to the perovskite phase and stabilizes it at appreciably lower pressures than the pure MgSiO$_3$ end-member. The effect of iron on the seismic properties of the post-perovskite phase is unknown.

[3] The exact amount, location, valence and spin state of iron in MgSiO$_3$ perovskite in the lower mantle is still not fully resolved. Experimental work has shown that perovskite containing a few mole percent Al$_2$O$_3$, as expected in the lower mantle, exhibits a Fe/(Fe + Mg) ratio of 0.11 [Wood and Rubie, 1996]. Of the iron incorporated, it is estimated that up to fifty percent is ferric, the rest being ferrous [McCammon, 1997]. Both are thought to substitute into the pseudo-dodecahedral magnesium sites, with ferric iron charge-balanced by aluminum in octahedral silicon sites [Miyajima et al., 2004]. Further studies, performed at room temperature, suggest that although ferric iron in perovskite is low-spin above pressures of 70 GPa, ferrous iron remains high-spin up to 120 GPa [Jackson et al., 2005], leading to a two-stage spin transition [Badro et al., 2004]. Since the effect of temperature would be to increase the transition pressures, one could therefore expect ferrous iron in perovskite to remain high-spin until the post-perovskite phase transition.

[4] In order to calculate the effect that incorporation of iron would have on the elastic and seismic properties of the perovskite and post-perovskite phases of MgSiO$_3$, we consider the pure FeSiO$_3$ end-members, with ferrous iron substituting for magnesium. This may be a hypothetical system, but it is useful in allowing us to estimate the effect of ferrous iron on the elastic properties. In conjunction with our results and analogous data calculated previously for the perovskite and post-perovskite phases of MgSiO$_3$ [Stackhouse et al., 2005a] and Al$_2$O$_3$ [Stackhouse et al., 2005b] we estimate the phase transition pressure and seismic properties of MgSiO$_3$ perovskite and post-perovskite phases containing realistic FeSiO$_3$ and Al$_2$O$_3$ mole fractions and discuss their possible geophysical implications.

2. Computational Details

[5] Calculations were performed in an identical manner to those in previous work [Stackhouse et al., 2005a], using the projector-augmented-wave (PAW) implementation [Blöchl, 1994; Kresse and Joubert, 1999] of the density functional theory based VASP code [Kresse and Furthmüller, 1996a, 1996b]. The exchange-correlation functional used adhered to the PW91 form of the generalized gradient approximation [Wang and Perdew, 1991; Perdew et al., 1992]. Twenty atom unit cells of the perovskite and post-perovskite polymorphs of pure end-member FeSiO$_3$ were structurally optimized at several pressures in the range 80–160 GPa, using a plane-
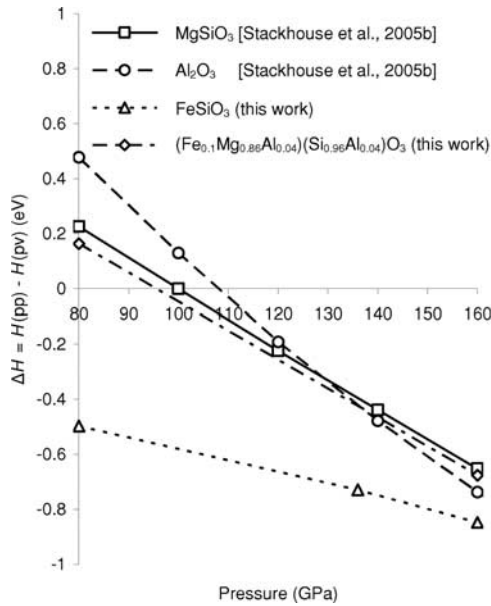
Figure 1. Static enthalpy difference for the perovskite and post-perovskite phases of pure end-member $FeSiO_3$, $MgSiO_3$ and Al_2O_3 as a function of pressure.

wave cut-off of 800 eV and sampling the Brillouin zone using Monkhorst-Pack grids [*Monkhorst and Pack*, 1976] of $6 \times 6 \times 6$ for the perovskite phase and $6 \times 6 \times 4$ for the post-perovskite phase.

[6] Our calculations show that for both the perovskite and post-perovskite phases of pure end-member $FeSiO_3$ a high-spin anti-ferromagnetic structure is energetically most favorable at all pressures. The low-spin phases were dynamically unstable, making it impossible to calculate their elastic constants. Studies of perovskite containing only ten mole percent $FeSiO_3$ show that it exhibits a low-spin structure at room temperature and 136 GPa [*Badro et al.*, 2004; *Li et al.*, 2004], but at lower mantle temperatures it may be predominantly high-spin. In addition, while the spin state of iron in magnesiowüstite is reported to greatly affect its bulk modulus [*Lin et al.*, 2005], our initial work on perovskite and post-perovskite phases of $MgSiO_3$ containing 6.25 mole percent $FeSiO_3$, which are dynamically stable in the low-spin state, show that the spin-state of ferrous iron changes their athermal elastic constants by under one percent (S. Stackhouse et al., manuscript in preparation, 2006), similar to results for ferric iron [*Li et al.*, 2005]. The results that follow, therefore, refer to high-spin states.

[7] To determine athermal elastic constants at 136 GPa, three different orthorhombic and one triclinic strains, of magnitude ±0.3, ±0.7 and ±1.0 percent were applied to the optimized models, the induced stresses calculated and resultant stress-strain relations fitted to a second-order polynomial. Single-crystal wave velocities were calculated from corresponding elastic constants by solving the Christoffel matrix [*Musgrave*, 1970]. Single-crystal elasticities were converted to transversely isotropic symmetries using the method outlined by *Wentzcovitch et al.* [1998].

[8] Increasing the plane-wave cut-off to 1000 eV and the Monkhorst-Pack grids by two **k**-points in each direction caused the calculated enthalpy difference of the two phases

to change by less than 1.0 meV per atom and the absolute value of the elastic constants to differ by an average of 0.1 percent.

3. Results and Discussion

[9] The enthalpy difference of the perovskite and post-perovskite phases of pure end-member $FeSiO_3$ over the pressure range $80-160$ GPa, is presented in Figure 1, with analogous data for pure end-member $MgSiO_3$ and Al_2O_3 shown for comparison. The calculated perovskite to post-perovskite phase transition pressures are expected to be lower than those observed experimentally as they neglect thermal effects. High-temperature calculations within the quasi harmonic approximation show that for pure end-member $MgSiO_3$ the phase transition pressure increases by about 30 GPa when determined at 4000 K [*Tsuchiya et al.*, 2004].

[10] The theoretical perovskite to post-perovskite phase transition pressure for pure end-member $FeSiO_3$ is about -35 GPa, which is over 135 GPa lower than that for pure end-member $MgSiO_3$ and 145 GPa lower than that for pure end-member Al_2O_3. This implies that it is more favorable for iron to enter the post-perovskite phase than the perovskite phase of $MgSiO_3$ at all real pressures and therefore iron will significantly reduce the perovskite to post-perovskite phase transition pressure. This agrees with the observations of *Mao et al.* [2004].

[11] If we assume linear mixing then we can calculate the static enthalpy difference of perovskite and post-perovskite polymorphs of $MgSiO_3$ incorporating four mole percent Al_2O_3 and ten mole percent $FeSiO_3$. While non-ideal mixing may be important, this gives a useful first-order estimate. Our results suggest that such an assemblage would exhibit a perovskite to post-perovskite phase transition pressure of about 95 GPa, which is 5.0 GPa lower than that seen for pure end-member $MgSiO_3$. Taking temperature into account, the transition pressure would increase by about 30 GPa at 4000 K, to give 125 GPa, which corresponds well with the top of the D″ layer, where the seismic discontinuity is observed [*Sidorin et al.*, 1999]. The small increase in phase transition pressure due to incorporation of aluminum [*Stackhouse et al.*, 2005b] is negligible, compared to the reduction affected by iron.

[12] Elastic constants calculated for the perovskite and post-perovskite phases of $FeSiO_3$ are listed in Table 1, with corresponding unit cell parameters, volumes and densities given in Table 2, and calculated shear-wave splitting for selected propagation directions listed in Table 3. Previous studies have shown that temperature can effect the degree of shear-wave splitting in a given propagation direction [*Stackhouse et al.*, 2005a], therefore high temperature calculations need to be done before we can be sure of their significance in the mantle. Here we note only that the shear-wave splitting exhibited by the post-perovskite phases of

Table 1. Calculated Elastic Moduli of Perovskite and Post-Perovskite Polymorphs of $FeSiO_3$ at 136 GPa and 0 K (in GPa)

	C_{11}	C_{22}	C_{33}	C_{12}	C_{13}	C_{23}	C_{44}	C_{55}	C_{66}	K	G
Perovskite	1036	1120	1165	600	494	552	324	227	263	732	272
Post-Perovskite	1174	993	1236	543	486	550	192	221	320	725	261

Table 2. Calculated Cell Parameters of Perovskite and Post-Perovskite Polymorphs of $FeSiO_3$ at 136 GPa and 0 K

	$a/Å$	$b/Å$	$c/Å$	$V/Å^3$	$\rho/kg\ m^{-3}$
Perovskite	4.384	4.601	6.300	127.05	6898
Post-Perovskite	2.439	8.380	6.170	126.16	6947

$FeSiO_3$ and $MgSiO_3$ are relatively similar. We suggest, therefore, that incorporating iron into $MgSiO_3$ post-perovskite will not significantly affect the shear-wave splitting exhibited by the phase, previously shown to be compatible with seismic observations [*Stackhouse et al.*, 2005a].

[13] The potential geophysical implications of these results depend, however, on how the crystals would align themselves via lattice preferred orientation. Some evidence exists for the core-mantle boundary layer being transversely isotropic in some regions [*Moore et al.*, 2004]. It is therefore useful to determine the seismic anisotropy of transversely isotropic aggregates of the perovskite and post-perovskite polymorphs of end-member $FeSiO_3$, listed in Table 4. It can be seen that shear-wave splitting exhibited by aggregates of the post-perovskite phase of $FeSiO_3$ is similar to that calculated for the analogous $MgSiO_3$ aggregates. Those with symmetry axes along [001] and [010] exhibit shear-wave splitting with polarization $V_{SH} > V_{SV}$, as is generally seen in the lowermost mantle [*Panning and Romanowicz*, 2004]. The most obvious slip-plane, that parallel to the silicate layers, would yield a transversely isotropic aggregate with a symmetry axis along the [010] direction, in accord with observations. It would, however, require a large degree of alignment, much more than for an aggregate with a symmetry axis along [001]. The definitive slip system for the post-perovskite phase, however, is yet to be confirmed.

[14] The bulk seismic velocities of the perovskite and post-perovskite polymorphs of $FeSiO_3$, $MgSiO_3$ and Al_2O_3 are listed in Table 5. The significance of these for the $MgSiO_3$ and Al_2O_3 phases have been discussed elsewhere [*Stackhouse et al.*, 2005b]. In the case of $FeSiO_3$ a 1.3 percent decrease is seen in compressional-wave speed and a 2.4 percent decrease in shear-wave speed, when going from the perovskite to post-perovskite phase. This is in contrast to the few percent increase in shear-wave speed observed for the post-perovskite transition in pure $MgSiO_3$ [*Stackhouse et al.*, 2005a] and similar increase in shear-wave speed observed in places atop of the core-mantle boundary layer, where the phase transition is expected to

Table 3. Calculated Shear Wave Splitting $((V_{S1} - V_{S2})/\langle V_S \rangle)*100$ for Perovskite and Post-Perovskite Polymorphs of $FeSiO_3$ [and $MgSiO_3$], at 136 GPa and 0 K, in Various Propagation Directions[a]

100	010	001	110	111
Perovskite Polymorph of FeSiO₃ [and MgSiO₃][b]				
7.0	10.8	17.8	7.0	10.7
[14.3]	[0.9]	[15.2]	[10.4]	[12.9]
Post-Perovskite Polymorph of FeSiO₃ [and MgSiO₃][c]				
18.7	25.1	6.4	12.4	16.3
[23.2]	[21.3]	[2.0]	[8.8]	[21.1]

[a]Note that V_{S1} is taken to be the faster than V_{S2} in each case.
[b]Taken from *Wookey et al.* [2005].
[c]Taken from *Stackhouse et al.* [2005a].

Table 4. Seismic Wave Velocity Anisotropy for Transversely Isotropic Aggregates, at 136 GPa and 0 K, of the Perovskite and Post-Perovskite Polymorphs of $FeSiO_3$ [and $MgSiO_3$] with Symmetry Axis Along the [100], [010] and [001] Directions[a]

	[001]	[010]	[100]
Perovskite Polymorph of FeSiO₃ [and MgSiO₃][b]			
Compressional	−3.4	−2.6	5.5
	[−1.7]	[−8.2]	[11.8]
Shear	−4.6	−5.2	11.7
	[−1.2]	[−11.9]	[7.4]
Post-Perovskite Polymorph of FeSiO₃ [and MgSiO₃][c]			
Compressional	−5.7	6.7	−4.8
	[−4.5]	[10.1]	[−7.8]
Shear	17.4	6.4	−6.6
	[16.3]	[1.9]	[−8.5]

[a]Note that a positive value infers that the horizontally polarized wave travels faster than that vertically polarized and vice versa.
[b]Taken from *Wookey et al.* [2005].
[c]Taken from *Stackhouse et al.* [2005a].

occur [*Sidorin et al.*, 1998]. If we can assume linear mixing of densities, bulk and shear moduli, from this and previous work [*Stackhouse et al.*, 2005a, 2005b; *Wookey et al.*, 2005] we can estimate possible bulk speeds for perovskite and post-perovskite polymorphs of $MgSiO_3$ containing both four mole percent Al_2O_3 and ten mole percent $FeSiO_3$, listed in Table 5. Note again, that non-linear mixing may well be important, but nevertheless this gives a useful first-order estimate. For such an assemblage, when going from perovskite to post-perovskite there is almost no change in compressional-wave speed, whereas the shear-wave speed increases by 1.8 percent and the bulk sound speed decreases by 0.5 percent. These values are consistent with the few percent increase in shear-wave speed observed in places atop of the core-mantle boundary [*Sidorin et al.*, 1998] and the anti-correlation of bulk sound and shear-wave speeds seen in the lowermost mantle [*Su and Dziewonski*, 1997; *Trampert et al.*, 2004].

[15] It has been proposed that ultra-low velocity zones observed in places at the base of the lower mantle may

Table 5. Density (ρ) (in kg m^{-3}), Compressional (V_P), Shear (V_S) and Bulk (V_Φ) Isotropic Wave Velocities (in km s^{-1}) of the Perovskite and Post-Perovskite Polymorphs of $FeSiO_3$, $MgSiO_3$ and Al_2O_3 at 136 GPa and 0 K

	ρ	V_P	V_S	V_Φ
Perovskite Polymorph				
$FeSiO_3$	6898	12.6	6.27	10.3
$MgSiO_3$[a]	5454	14.4	7.73	11.3
Al_2O_3[b]	5477	13.9	7.22	11.2
$(Fe_{0.1}Mg_{0.86}Al_{0.04})(Si_{0.96}Al_{0.04})O_3$[c]	5599	14.2	7.55	11.2
$(Fe_{0.5}Mg_{0.46}Al_{0.04})(Si_{0.96}Al_{0.04})O_3$[c]	6177	13.4	6.94	10.8
Post-Perovskite Polymorph				
$FeSiO_3$	6947	12.4	6.13	10.2
$MgSiO_3$[d]	5528	14.5	7.91	11.2
Al_2O_3[b]	5577	14.0	7.09	11.3
$(Fe_{0.1}Mg_{0.86}Al_{0.04})(Si_{0.96}Al_{0.04})O_3$[c]	5671	14.2	7.68	11.1
$(Fe_{0.5}Mg_{0.46}Al_{0.04})(Si_{0.96}Al_{0.04})O_3$[c]	6239	13.4	6.94	10.7

[a]Taken from *Wookey et al.* [2005].
[b]Taken from *Stackhouse et al.* [2005b].
[c]Estimated from linear mixing of densities, bulk and shear moduli of other phases.
[d]Taken from *Stackhouse et al.* [2005a].

comprise iron-enriched material [*Dobson and Brodholt*, 2005] in particular post-perovskite [*Mao et al.*, 2004]. The generally observed decrease in compressional and shear-wave speed in ultra-low velocity zones is 5−10 percent [*Garnero and Helmberger*, 1995; *Williams and Garnero*, 1996], although larger decreases of 8 percent for compressional-waves and 25 percent for shear-waves have recently been observed east of Australia [*Rost et al.*, 2005]. Using linear mixing we estimate that increasing the mole percentage of $FeSiO_3$ incorporated into $MgSiO_3$ post-perovskite from ten to fifty would result in an increase in density of about 10.0 percent and a decrease in compressional and shear-wave velocities of about 6.1 and 9.6 percent. This is in reasonable agreement with most observations, but not those of the ultra-low velocity zone seen east of Australia, which is suggested to arise due to melt [*Rost et al.*, 2005].

[16] In conclusion, the incorporation of ten mole percent $FeSiO_3$ into $MgSiO_3$ is predicted to slightly reduce the perovskite to post-perovskite transition pressure. Small changes in the seismic properties of the post-perovskite phase due to incorporation of iron and aluminum are compatible with observations for the lowermost mantle. $MgSiO_3$ post-perovskite enriched by fifty mole percent $FeSiO_3$ may be responsible for ultra-low velocity zones at the base of the lower mantle.

References

Anderson, D. L. (1989), *Theory of the Earth*, 148 pp, Blackwell Sci., Malden, Mass.

Badro, J., J.-P. Rueff, G. Vankó, G. Monaco, G. Fiquet, and F. Guyot (2004), Electronic transitions in perovskite: Possible nonconvecting layers in the lower mantle, *Science*, 305, 383–386.

Blöchl, P. R. (1994), Projector augmented-wave method, *Phys. Rev. B.*, 50, 17,953–17,979.

Caracas, R., and R. E. Cohen (2005), Prediction of a new phase transition in Al_2O_3 at high pressures, *Geophys. Res. Lett.*, 32, L06303, doi:10.1029/2004GL022204.

Dobson, D., and J. P. Brodholt (2005), Subducted banded iron formations as a source of ultralow-velocity zones at the core-mantle boundary, *Nature*, 434, 371–374.

Garnero, E. J., and D. V. Helmberger (1995), A very low basal layer underlying large-scale low-velocity anomalies in the lower mantle beneath the Pacific: Evidence from core phases, *Phys. Earth Planet Inter.*, 91, 161–176.

Iitaka, T., K. Hirose, K. Kawamura, and M. Murakami (2004), The elasticity of the $MgSiO_3$ post-perovskite phase in the Earth's lowermost mantle, *Nature*, 430, 442–445.

Jackson, J. M., W. Sturhahn, G. Shen, J. Zhao, M. Y. Hu, D. Errandonea, J. D. Bass, and Y. Fei (2005), A synchrotron Mössbauer spectroscopy study of (Mg,Fe)SiO_3 perovskite up to 120 GPa, *Am. Mineral.*, 90, 199–205.

Kresse, G., and J. Furthmüller (1996a), Efficient interative schemes for ab initio total-energy calculations using a plane-wave basis set, *Phys. Rev. B*, 54, 11,169–11,186.

Kresse, G., and J. Furthmüller (1996b), Efficiency of ab initio total energy calculations for metals and semiconductors using a plane-wave basis set, *Comput. Mat. Sci.*, 6, 15–50.

Kresse, G., and D. Joubert (1999), From ultrasoft pseudopotentials to the projector augmented-wave method, *Phys. Rev. B*, 59, 1758–1775.

Lay, T., E. J. Garnero, and Q. Williams (2004), Partial melting in a thermo-chemical boundary layer at the base of the mantle, *Phys. Earth Planet. Inter.*, 146, 441–467.

Li, J., V. V. Struzhkin, H.-W. Mao, J. Shu, R. J. Hemley, Y. Fei, B. Mysen, P. Dera, V. Prakapenka, and G. Shen (2004), Electronic spin state of iron in lower mantle perovskite, *Proc. Natl. Acad. Sci.*, 101, 14,027–14,030.

Li, L., J. P. Brodholt, S. Stackhouse, D. Weidner, M. Alfredsson, and G. D. Price (2005), Elasticity of (Mg, Fe) (Si, Al)O_3-perovskite at high pressure, *Earth Planet. Sci. Lett.*, 240, 529–536.

Lin, J.-F., V. V. Struzhkin, S. D. Jacobsen, M. Y. Hu, P. Chow, J. Kung, H. Liu, H.-K. Mao, and R. J. Hemley (2005), Spin transition of iron in magnesiowüstite in the Earth's lower mantle, *Nature*, 436, 377–380.

Mao, W. L., G. Shen, V. B. Prakapenka, Y. Meng, A. J. Campbell, D. L. Heinz, J. Shu, R. J. Hemley, and H.-K. Mao (2004), Ferromagnesian post-perovskite silicates in the D″ Layer, *Proc. Natl. Acad. Sci.*, 101, 15,867–15,869.

McCammon, C. (1997), Perovskite as a possible sink for ferric iron in the lower mantle, *Nature*, 387, 694–696.

Miyajima, N., F. Langenhorst, D. J. Frost, and T. Yagi (2004), Electron channeling spectroscopy of iron in majoritic garnet and silicate perovskite using a transmission electron microscope, *Phys. Earth. Planet. Inter.*, 143–144, 601–609.

Monkhorst, H. J., and J. D. Pack (1976), Special points for Brillouin-zone integrations, *Phys. Rev. B*, 13, 5188–5192.

Moore, M. M., E. J. Garnero, T. Lay, and Q. Williams (2004), Shear wave splitting and waveform complexity for lowermost mantle structures with low-velocity lamellae and transverse isotropy, *J. Geophys. Res.*, 109, B02319, doi:10.1029/2003JB002546.

Murakami, M., K. Hirose, K. Kawamura, N. Sata, and Y. Ohishi (2004), Post-perovskite phase transition in $MgSiO_3$, *Science*, 304, 855–858.

Musgrave, M. J. P. (1970), *Crystal Acoustics*, Holden-Day, Boca Raton, Fla.

Oganov, A. R., and S. Ono (2004), Theoretical and experimental evidence for a post-perovskite phase of $MgSiO_3$ in Earth's D″ layer, *Nature*, 430, 445–448.

Panning, M., and B. Romanowicz (2004), Inferences on flow at the base of Earth's mantle based on seismic anisotropy, *Science*, 303, 351–353.

Perdew, J. P., J. A. Chevary, S. H. Vosko, K. A. Jackson, M. R. Pederson, D. J. Singh, and C. Fiolhais (1992), Atoms, molecules, solids, and surfaces–applications of the generalized gradient approximation for exchange and correlation, *Phys. Rev. B*, 46, 6671–6687.

Rost, S., E. J. Garnero, Q. Williams, and M. Manga (2005), Seismological constraints on a possible plume root at the core-mantle boundary, *Nature*, 435, 666–669.

Shim, S.-H., T. S. Duffy, R. Jeanloz, and G. Shen (2004), Stability and crystal structure of $MgSiO_3$ perovskite to the core-mantle boundary, *Geophys. Res. Lett.*, 31, L10603, doi:10.1029/2004GL019639.

Sidorin, I., M. Gurnis, D. V. Helmberger, and X. Ding (1998), Interpreting D″ seismic structure using synthetic waveforms computed from dynamic models, *Earth Planet. Sci. Lett.*, 163, 31–41.

Sidorin, I., M. Gurnis, and D. V. Helmberger (1999), Evidence for a ubiquitous seismic discontinuity at the base of the mantle, *Science*, 286, 1326–1331.

Stackhouse, S., J. P. Brodholt, J. Wookey, J.-M. Kendall, and G. D. Price (2005a), The effect of temperature on the seismic anisotropy of the perovskite and post-perovskite polymorphs of $MgSiO_3$, *Earth Planet. Sci. Lett.*, 230, 1–10.

Stackhouse, S., J. P. Brodholt, and G. D. Price (2005b), High temperature elastic anisotropy of the perovskite and post-perovskite polymorphs of Al_2O_3, *Geophys. Res. Lett.*, 32, L13305, doi:10.1029/2005GL023163.

Su, W.-J., and A. M. Dziewonski (1997), Simultaneous inversion for 3−D variations in shear and bulk velocity in the mantle, *Phys. Earth Planet. Inter.*, 100, 135–156.

Trampert, J., F. Deschamps, J. Resovsky, and D. Yuen (2004), Probabilistic tomography maps chemical heterogeneities throughout the lower mantle, *Science*, 306, 853–856.

Tsuchiya, T., J. Tsuchiya, K. Umemoto, and R. M. Wentzcovitch (2004), Phase transition in $MgSiO_3$ perovskite in the Earth's lower mantle, *Earth. Planet. Sci. Lett.*, 224, 241–248.

Wang, Y., and J. P. Perdew (1991), Correlation hole of the spin-polarized electron-gas, with exact small-wave-vector and high density scaling, *Phys. Rev. B*, 44, 13,298–13,307.

Wentzcovitch, R. M., B. B. Karki, S. Karoto, and C. R. S. Da Silva (1998), High pressure elastic anisotropy of $MgSiO_3$ perovskite and geophysical implications, *Earth Planet. Sci. Lett.*, 164, 371–378.

Williams, Q., and E. J. Garnero (1996), Seismic evidence for partial melt at the base of Earth's mantle, *Science*, 273, 1528–1530.

Wood, B. J., and D. C. Rubie (1996), The effect of alumina on phase transformations at the 660–kilometer discontinuity from Fe-Mg partitioning experiments, *Science*, 273, 1522–1524.

Wookey, J., S. Stackhouse, J.-M. Kendall, J. P. Brodholt, and G. D. Price (2005), Efficacy of post-perovskite as an explanation for lowermost mantle seismic properties, *Nature*, 438, 1004–1007.

―――――――――――

   J. P. Brodholt, G. D. Price, and S. Stackhouse, Department of Earth Sciences, University College London, Gower Street, London WC1E 6BT, UK. (s.stackhouse@ucl.ac.uk)